University of Wollongong

Research Online

2019

Modelling the Biological Beamline at HIMAC using Geant4

David Bolst
University of Wollongong, dbolst@uow.edu.au

Linh T. Tran
University of Wollongong, tltran@uow.edu.au

Susanna Guatelli
University of Wollongong, susanna@uow.edu.au

Naruhiro Matsufuji
National Institute Of Radiological Sciences, matufuji@nirs.go.jp

Anatoly B. Rosenfeld
University of Wollongong, anatoly@uow.edu.au

Recommended Citation

Modelling the Biological Beamline at HIMAC using Geant4

Abstract

A Geant4 simulation modelling the passive Biological beamline at the Heavy Ion Medical Accelerator Chiba (HIMAC) is described and validated against experimental measurements for a mono-energetic and spread out Bragg peak (SOBP) ^{12}C beam. Comparisons to experimental data showed good agreement for both lateral and depth dose profiles. It was found that simplifying the simulation model by generating a cone beam instead of using the wobbler magnets provided a good approximation for both lateral and depth dose measurements.

Disciplines

Engineering | Science and Technology Studies

Publication Details

PAPER • OPEN ACCESS

Modelling the Biological Beamline at HIMAC using Geant4

To cite this article: D Bolst *et al* 2019 *J. Phys.: Conf. Ser.* **1154** 012003

View the article online for updates and enhancements.

Modelling the Biological Beamline at HIMAC using Geant4

D Bolst[1]**, L T Tran**[1]**, S Guatelli**[1]**, N Matsufuji**[2] **and A B Rosenfeld**[1]
[1]Centre for Medical Radiation Physics, University of Wollongong, Australia
[2]Research Centre for Charge Particle Therapy, National Institute of Radiological Science, Chiba, Japan

E-mail: db001@uowmail.edu.au

Abstract. A Geant4 simulation modelling the passive Biological beamline at the Heavy Ion Medical Accelerator Chiba (HIMAC) is described and validated against experimental measurements for a mono-energetic and spread out Bragg peak (SOBP) ^{12}C beam. Comparisons to experimental data showed good agreement for both lateral and depth dose profiles. It was found that simplifying the simulation model by generating a cone beam instead of using the wobbler magnets provided a good approximation for both lateral and depth dose measurements.

1. Introduction

The Heavy Ion Medical Accelerator (HIMAC) at the National Institute of Radiological Sciences (NIRS), in Chiba, Japan, was the first centre to clinically treat patients with ^{12}C and as of 2015 has treated more than 10000 patients with ^{12}C therapy [1]. Since then, ^{12}C therapy has had a growing interest thanks to its enhanced physical and biological dose properties, however, the ^{12}C beam produces a complex radiation field which needs to be fully characterised for Quality Assurance. Monte Carlo simulations are a very useful tool supporting the research in ^{12}C ion therapy, however, simulations must be validated against experimental data to quantify their predictive accuracy. In this work the modelling of the Biological beamline at HIMAC using Geant4 is described and validated against experimental measurements. This simulation model is used at the Centre for Medical Radiation Physics, University of Wollongong, to study novel detector solutions for Quality Assurance including silicon micro dosimeters [2-4].

2. Materials and Methods

2.1. Simulation Setup

The Biological beamline was modelled in Geant4 [5, 6] using version 10.2p2. The layout of the modelled beamline can be seen in figure 1. The ^{12}C beam is generated at the beam duct in a vacuum tube 205 cm in length. The ^{12}C beam has an initial energy of 290 MeV/u and a 0.2% energy σ. The beam is generated as a Gaussian distribution with a spot size of 3.4 mm σ.
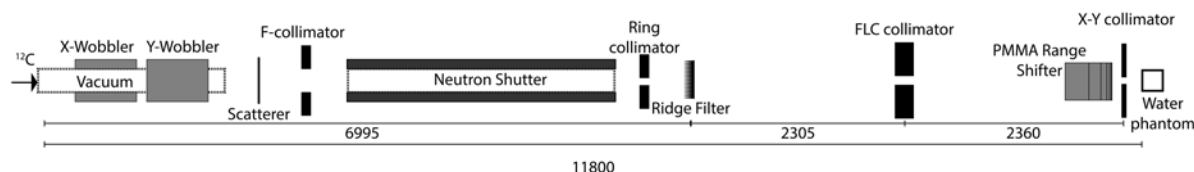

Figure 1. Layout of the Biological beamline modelled in Geant4, not to scale.

The beam is then shaped to a circle by two wobbler magnets operated using the single-ring wobbling method [7]. The strength of the magnetic field at a particular time t is $B_0 \sin(\omega t)$ and $B_0 \cos(\omega t)$ for the X and Y wobbler magnets respectively, where ω is 56.41 Hz. In the simulation the period is sampled at 111 different times. Each wobbler magnet is modelled as a cylinder with a radius of 250 mm and length of 660.1 mm with a 110 mm gap between the two wobbler magnets. In the simulation a uniform magnetic field is applied to both the wobbler magnets.

Once the beam is shaped by the pair of wobbler magnets the lateral dose uniformity of the beam is improved by passing through a tantalum scatterer which is located at ~2308 mm from the beam duct. The thickness of the scatterer and wobbler strength, B_0, depend on the energy and ion of the beam being delivered, as well as the field size. For the mono-energetic 290 MeV/u ^{12}C beam the B_0 is 0.045 T and the scatterer is 0.434 mm thick while the SOBP has a B_0 of 0.061 T and a scatterer thickness of 0.649 mm.

After passing through the scatterer, the beam is collimated by a 100 mm thick brass F-collimator with a diameter of 100 mm, located 2755 mm from the beam duct. After the F-collimator the contribution of neutrons in the beam is reduced by traversing a 2885 mm long vacuum neutron shutter. After exiting the neutron shutter, the beam is further collimated by a 200 mm thick brass ring collimator with a diameter of 100 mm.

In the SOBP configuration, the beam will then pass through a ridge filter (RGF), located 6995 mm from the beam duct. For a 6 cm 290 MeV/u ^{12}C SOBP the RGF is made up of 21 bars of milled aluminium 200 mm in length and ~5 mm wide, each bar consists of 101 different thicknesses.

The beam then traverses a 20 cm thick aluminium, four leaf collimator (FLC) placed 9300 mm from the beam duct. The beam can then pass through various combinations of PMMA thicknesses to shift the range of the beam, though none are used in this study. The beam can then be further collimated by a 5 cm thick X-Y brass collimator, 140 mm before isocentre.

The changing shape of the beam as it traverses the beamline is shown in figure 2, which shows the transport of ~10^4 mono-energetic ^{12}C ions from the beam duct to the isocentre with a field size of 100×100 mm^2 set by the collimators.

In the Geant4 simulation after the final brass collimator there is the option to generate a phase space file (PSF) by recording particle details in a ROOT file such as the particle type (ion, neutron, electron or photon). If the particle type is an ion, then the A and Z will also be stored. Each particle's x, y, z position and momentum are also stored along with its kinetic energy. When reading in the PSF, 1000 entries are read into memory at a time to increase the speed of the simulation.

In this study two phantom sizes were used for scoring the lateral and depth doses with sizes of $30 \times 30 \times 30$ cm^3 and $22 \times 22 \times 30$ cm^3 respectively, where 30 cm is the thickness for both cases. The phantom size of 22×22 cm^2 was used to match the size used in [8]. The scoring of the lateral dose profile was done in $5 \times 5 \times 10$ mm^3 voxels at the surface of the phantom. For calculating the depth dose, the phantom had 1 mm thick water cylinders with diameters of 10 mm placed along the beam axis.

There are various 10 μm thick aluminium sheets placed throughout the beamline. These represent ionisation chamber (IC) monitors and the end of the first vacuum chamber and the start and end of the neutron shutter. The IC are made up of two sheets of aluminium and are positioned at 2175, 6910, 6950 and 8525 mm from the beam duct.

To describe electromagnetic interactions the *G4StandardOption3* physics list was adopted. Hadronic interactions were modelled using the Binary Intranuclear Cascade (BIC) which has been recently benchmarked against other alternative models in Geant4 [9] for a therapeutic ^{12}C beam. The elastic scattering of hadrons was modelled by means of the *G4HadronElasticPhysicsHP* and the neutron High Precision (HP) model was adopted to describe neutron interactions of energies up to 20 MeV. Within the water phantom a production cut size and step limit of 0.5 mm were used.

In order to validate the Geant4 simulation both lateral and depth dose profiles were compared to experimental measurements. For a 290 MeV/u mono-energetic and 6 cm SOBP ^{12}C beam experimental data from [10] and [11] were used, respectively, for the lateral dose. For both these cases the dose is measured at the surface of the phantom with an ionisation chamber with the FLC and brass collimator being fully opened. For depth dose measurements data from [8] were used for both beams. For lateral dose comparisons the maximum value in the experiment and simulation were both normalised to the

same value, while for reference depth dose comparisons the first depth in the experiment was used to normalise the experiment and simulation distributions.
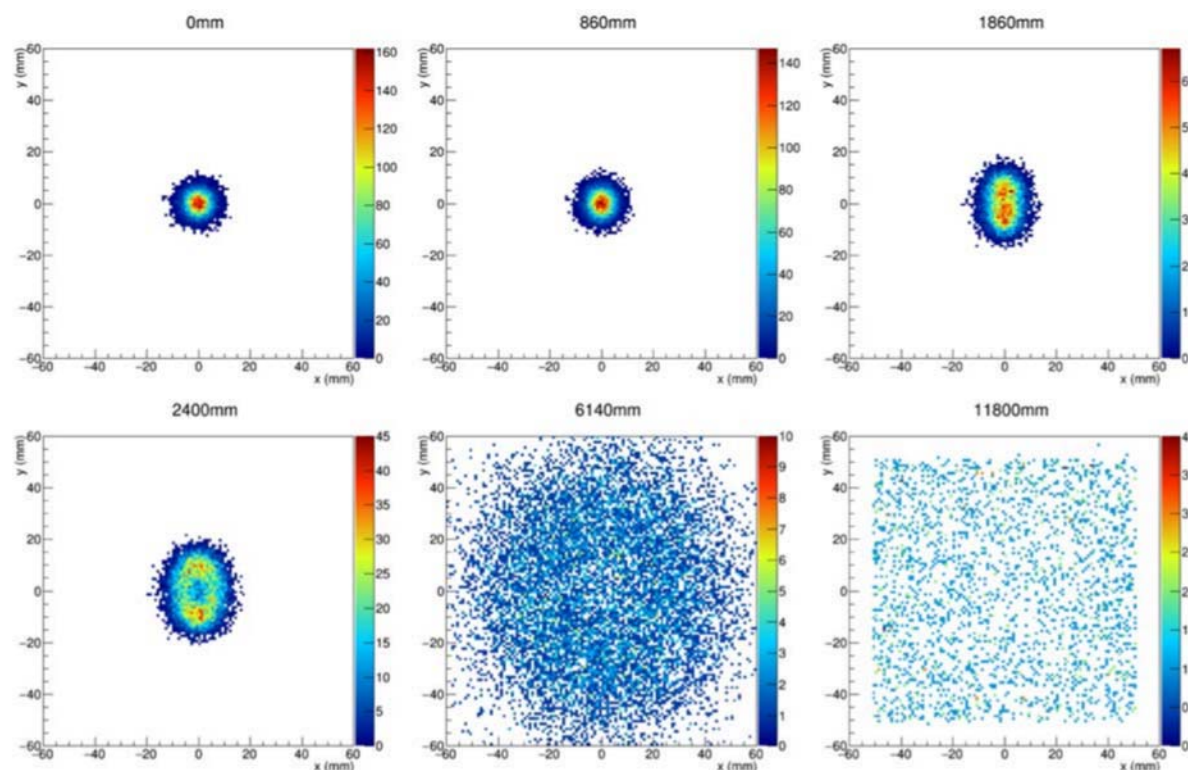

Figure 2 A beam's eye view of the fluence of a mono-energetic ^{12}C beam with ~10^4 primary particles at various distances from the beam duct. The 860 and 1860 mm positions correspond to the exit of the first and second wobbler magnets, respectively. The 2400 and 6140 mm distances show the profile of the beam after traversing the scatterer and neutron shutter, respectively. The 11800 distance is the profile at isocentre after being collimated to a 100×100 mm^2 size.

To investigate whether the simulation could be simplified by excluding the wobbler, the lateral and depth dose profiles were compared to the case of having the wobbler setup with the FLC and brass collimators set to a field size of 100 × 100 mm^2, a common field size of interest. The simplified methods consist of deactivating the wobbler magnets and generating the particles at the same beam duct position as used for the full wobbler technique. The different methods included simulating a 3.4 mm σ pencil beam (the same initial beam size used for the full wobbler method), a cone beam simulated by generating an isotropic distribution with an aperture angle of 1 degree and finally a circular beam with diameter of 100 mm and generated uniformly. A beam's eye view of the fluence using the different methods is shown in figure 3, the positions are at the beam duct where the beam is generated (0 mm) and just before the neutron shutter (3200 mm).
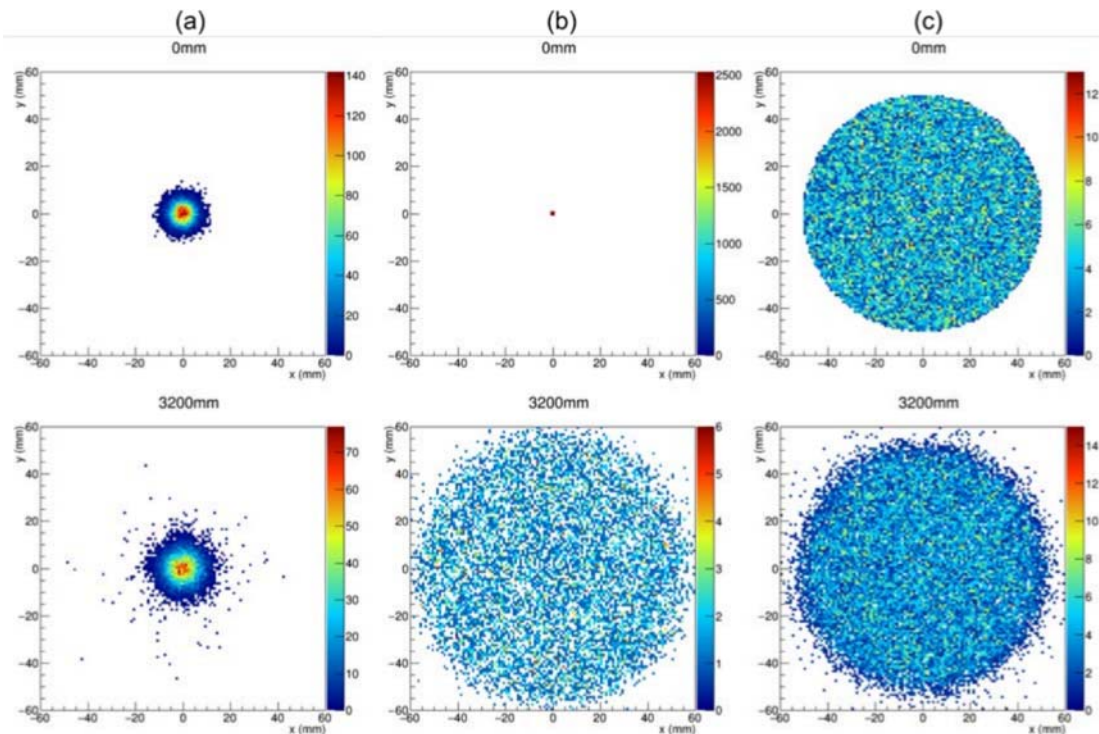
Figure 3. A beam's eye view of the fluence of the beam simulated with different methods at the beam duct (0 mm) and just before the neutron shutter (3200 mm). (a) 3.4 mm σ pencil beam, (b) 1° cone beam and (c) 100 mm diameter circle beam.

3. Results and Discussion

3.1. Validation

Figure 4 shows the comparison of simulation and experimental data in terms of the lateral and depth dose profiles with the percentage difference (PD) plotted at the bottom. The PD was calculated using equation (1). Overall, the agreement between simulation and experiment is satisfactory for both the lateral and depth dose profiles.

$$PD = \left(\frac{Exp - Sim}{Exp}\right) \times 100\% \tag{1}$$

The lateral dose profiles at the surface of the phantom are shown for a mono-energetic beam (a) and a SOBP (b). It can be seen that for the pristine beam there is excellent agreement between the experiment and simulation with a difference of less than 0.5% in the treatment field between ±50 mm. At the sharp penumbra the difference increases to a maximum of ~2.5%, however due to the rapidly changing dose in this region experimental positioning becomes more sensitive. For the SOBP there is visibly less agreement, with the treatment field varying between ~2%, however the penumbra gives agreements within ~1%.
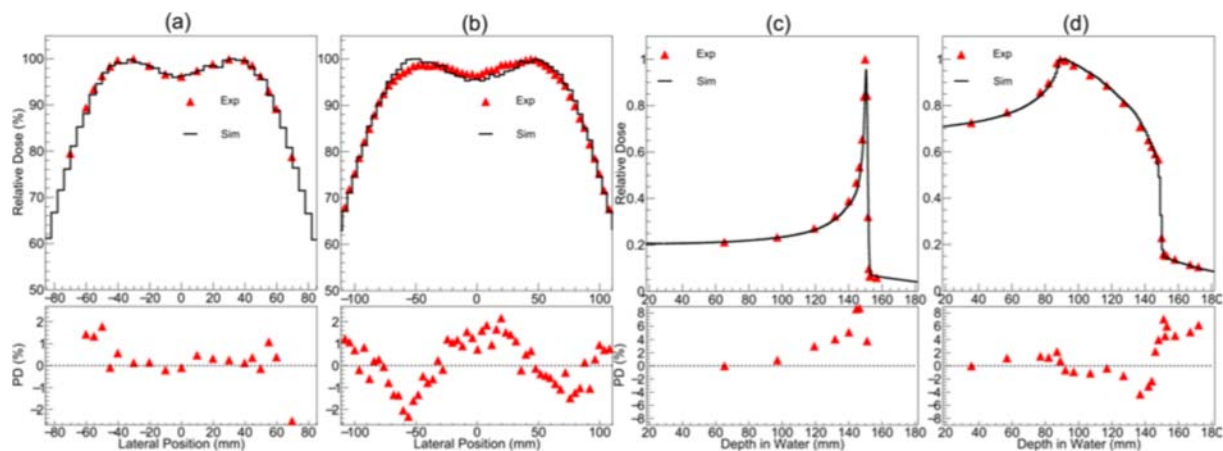
Figure 4. Comparison between the relative dose calculated by means of the simulation and experiment with the percentage difference (PD) plotted on the bottom. Plots (a) and (b) show the lateral dose at the surface of the phantom for a mono-energetic (a) and 6 cm SOBP (b) 290MeV/u ^{12}C beam. Plots (c) and (d) compare the depth dose distribution for the mono-energetic (c) and SOBP (d) beams.

The depth dose distributions for a mono-energetic and SOBP 290 MeV/u ^{12}C beam are shown in (c) and (d), respectively. Both setups are done using a collimation size of 100×100 mm^2 for both the FLC and brass collimator. For the mono-energetic beam the overall shape agrees very well, however the difference between the simulation and the experiment gradually increases with depth and has a maximum of ~8% at the pinnacle of the BP. The SOBP depth dose (d) shows a more stable difference between the simulation and the experiment with a difference between ~2%. Like with the mono-energetic beam the SOBP beam also has a maximum difference at the end of the SOBP range, these regions have sharp dose gradients and are sensitive to slight misplacements or energy differences of the delivered beam.

3.2. Simplified simulations techniques to model the effect of the wobbler
A comparison of the different simplified simulation techniques is shown in figure 5, with the plotted percentage differences being calculated with respect to the full wobbler method.

The lateral dose is compared using a mono-energetic beam collimated to a 100×100 mm^2 field and is shown in (a). It can be seen that the cone beam reproduces the lateral beam profile of the wobbler setup very well, with a difference within ~2% for the treatment field with the difference increasing at the penumbra, while both the point and circle beams agree very poorly.

The depth dose, using the different simulation techniques is shown in (b) for the mono-energetic beam and (c) for the SOBP. For the mono-energetic beam the different methods of modelling the beam do not vary strongly with one another, with the cone beam not differing significantly. The pencil and circle beams are very similar to one another, with them both increasing in difference with depth compared to the wobbler method, with a difference of ~1% higher at the pinnacle of the BP, after the BP they both under respond compared to the wobbler with a difference which increases with depth.

For the case of the SOBP (c), shows a much more prominent difference between the cone beam compared to the point and circle beams. Without the angular spread, the point and circular beams create a flatter dose over the range of the SOBP between 85 and 145 mm, with a maximum difference of ~15% at the end of the SOBP.
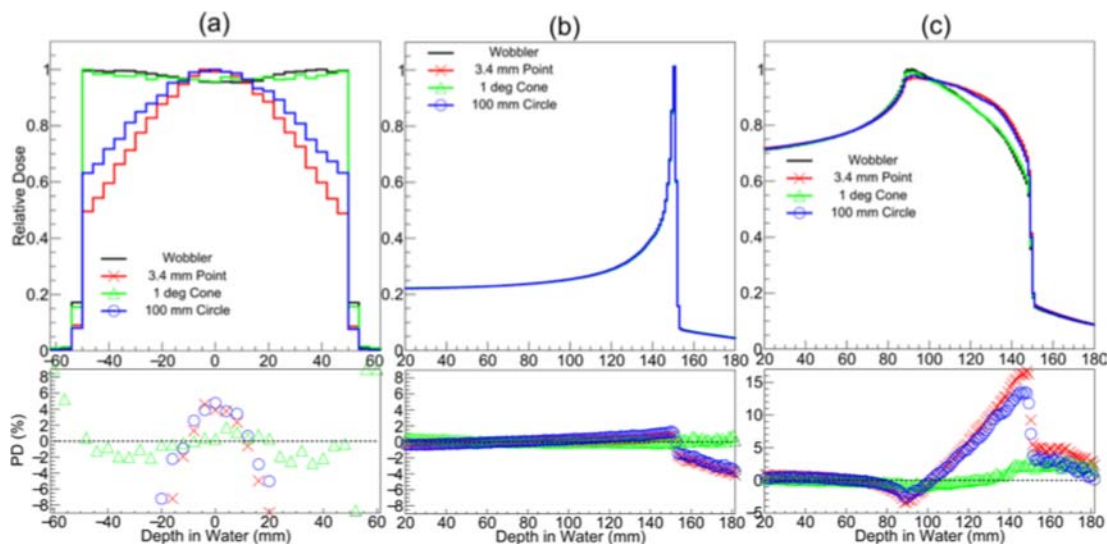
Figure 5. Comparison of the lateral dose for a mono-energetic beam (a) and the depth dose of a mono-energetic (b) and a SOBP (c) when using different methods to model the effect of the wobbler on the beam shape. The percentage difference (PD) is calculated with respect to the dose distributions using the wobbler simulation.

4. Conclusion

A Geant4 application modelling the Biological Beamline at HIMAC, NIRS, has been described and validated against experimental measurements for a mono-energetic and SOBP 290 MeV/u ^{12}C beam. Comparisons with experiment for the lateral beam profile showed good agreement for both mono-energetic and SOBP beams, with differences of ~0.5% and 2% in the treatment field, respectively. For the depth dose profiles, both beams gave good agreement in the overall shape, however both have a maximum difference with the experiment at the end of the BP where measurements are especially sensitive. In order to simplify the simulation by excluding the wobbler system a number of alternative methods were modelled. It was found that for both lateral and depth dose profiles simulating a cone beam provided very good agreement compared to modelling the full wobbler system.

5. References

[1]   https://www.ptcog.ch/
[2]   Bolst D *et al* 2017 *Rad. Meas. A* **106** 512-518
[3]   Chartier L *et al* 2017 *Rad. Prot. Dos.* **180** 365-71
[4]   Tran L *et al* 2018 *Med. Phys.* **44** 6085-6095
[5]   Agostinelli A et al 2003 *Nucl. Instr. Meth. Phys. Res. A* **506** 250-303
[6]   Allison J et al 2016 *Nucl. Instr. Meth. Phys. Res. A* **835** 186-225
[7]   Yonai S *et al* 2008 *Med. Phys.* **35** 2473-4209
[8]   Tran L *et al* 2018 *Radiat. Meas.* **115** 55-59
[9]   Bolst D et al 2017 *Nucl. Instr. Meth. Phys. Res. A* **869** 68-75
[10] http://wrmiss.org/workshops/sixteenth/Ploc.pdf
[11] Yonai S *et al* 2009 *Med. Phys.* **36** 927-938